Perturbation of Cell Adhesion and Microvilli Formation by Antisense Oligonucleotides to ERM Family Members

Kosei Takeuchi,*‡ Naruki Sato,*‡ Hideko Kasahara,*§ Noriko Funayama,* Akira Nagafuchi,* Shigenobu Yonemura,* Sachiko Tsukita,* and Shoichiro Tsukita*‡

* Laboratory of Cell Biology, Department of Information Physiology, National Institute for Physiological Sciences, and ‡ Department of Physiological Sciences, School of Life Sciences, The Graduate University of Advanced Studies, Aichi 444, Japan; and § First Department of Internal Medicine, Nagoya University School of Medicine, Nagoya 466, Japan

Abstract. To examine the functions of ERM family members (ezrin, radixin, and moesin), mouse epithelial cells (MTD-1A cells) and thymoma cells (L5178Y), which coexpress all of them, were cultured in the presence of antisense phosphorothioate oligonucleotides (PONs) complementary to ERM sequences. Immunoblotting revealed that the antisense PONs selectively suppressed the expression of each member. Immunofluorescence microscopy of these ezrin, radixin, or moesin "single-suppressed" MTD-1A cells revealed that the ERM family members are colocalized at cell–cell adhesion sites, microvilli, and cleavage furrows, where actin filaments are densely associated with plasma membranes. The ezrin/radixin/moesin antisense PONs mixture induced the destruction of both cell–cell and cell–substrate adhesion, as well as the disappearance of microvilli. Ezrin or radixin antisense PONs individually affected the initial step of the formation of both cell–cell and cell–substrate adhesion, but did not affect the microvilli structures. In sharp contrast, moesin antisense PONs did not singly affect cell–cell and cell–substrate adhesion, whereas it partly affected the microvilli structures. These data indicate that ezrin and radixin can be functionally substituted, that moesin has some synergetic functional interaction with ezrin and radixin, and that these ERM family members are involved in cell–cell and cell–substrate adhesion, as well as microvilli formation.

THE ERM family consists of three closely related proteins; ezrin, radixin, and moesin (Sato et al., 1992; Tsukita et al., 1992). Ezrin (also called cytovillin or p81) was first identified as a constituent of microvilli in intestinal epithelial cells (Bretscher, 1983; Pakkanen et al., 1987), and is a good substrate in vivo for tyrosine kinases such as EGF receptors (Bretscher, 1989; Gould et al., 1986; Hunter and Cooper, 1981, 1983). Radixin is an actin-modulating protein that was first purified and characterized from the isolated cell–cell adherens junction fraction (Tsukita et al., 1989). Moesin was originally identified as an extracellular heparin-binding protein (Lankes et al., 1988) and was later found to be intracellular (Lankes and Furthmayr, 1991). Since these proteins were very similar, the identity of each was not fully established until each cDNA was cloned and sequenced (Gould et al., 1989; Turunen et al., 1989; Funayama et al., 1991; Lankes and Furthmayr, 1991; Sato et al., 1992).

Sequence analyses revealed that these three proteins are highly homologous; in the mouse, the identity is 75, 72, and 80% for ezrin/radixin, ezrin/moesin, and radixin/moesin, respectively (Funayama et al., 1991; Sato et al., 1992). The sequence of their NH_2-terminal half is highly conserved (~85% identity for any pair). This sequence was also found in the NH_2-terminal region of the band 4.1 superfamily members such as band 4.1 protein, talin, and protein-tyrosine-phosphatases (PTPH1 and PTMEG), indicating that the ERM family is included in the band 4.1 superfamily (Conboy et al., 1986; Rees et al., 1990; Gu et al., 1991; Yang et al., 1991). Detailed analysis with in vitro translation using cDNAs revealed that mouse ezrin, radixin, and moesin migrate at 85, 82, 75 kD in SDS-PAGE, which allows the expression of these ERM family members in various types of cells and tissues to be compared by immunoblotting (Sato et al., 1992). In all types of mouse cultured cells so far examined, ezrin, radixin, and moesin are all coexpressed, but their expression profiles are distinct among tissues in vivo.

The distribution of ERM family members inside cells has been so far intensively analyzed using various combinations of antibodies and cells (Bretscher, 1983; Pakkanen et al., 1987; Tsukita et al., 1989; Lankes et al., 1988; Sato et al., 1991, 1992; Franck et al., 1993; Berryman et al., 1993). However, the results have not been consistent. This is probably because (*a*) the identity of each protein was confused, (*b*) the antibodies were not specific for each protein, and (*c*) the masking problem for immunofluorescence microscopy was

Address all correspondence to Shoichiro Tsukita, M.D., Department of Physiological Information, National Institute for Physiological Sciences, Myodaiji-cho, Okazaki, Aichi 444, Japan.

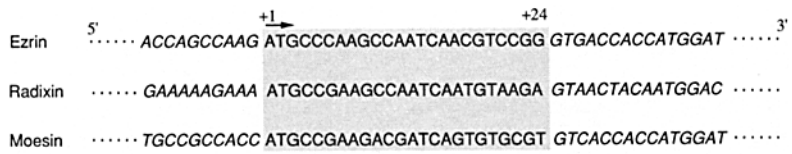

Figure 1. Nucleotide sequences (−10∼39; relative to the translation initiation site) of mouse ezrin, radixin, and moesin (Funayama et al., 1991; Sato et al., 1992). Antisense PONs complementary to position 1-24 of ezrin, radixin, and moesin were synthesized (*shadowed*). Sense PONs of this region were also synthesized as controls.

severe. Taking all localization studies of ERM family members into consideration, what we can conclude at present is that at least one ERM family member is concentrated in the plasmalemmal undercoat at microvilli, ruffling membranes, and cleavage furrows (Sato et al., 1992; Franck et al., 1993; Berryman et al., 1993). These are specialized sites where actin filaments are densely associated with plasma membranes; therefore, ERM family members may play a crucial role in the association between actin filaments and plasma membranes in general. This notion seems to be consistent with biochemical data. The NH_2-terminal half of band 4.1 protein, which shows similarity with the NH_2-terminal half of ERM family members, is responsible for its direct binding to an integral membrane protein called glycophorin C in erythrocytes (Anderson and Lovrien, 1984; Anderson and Marchesi, 1985; Leto et al., 1986), suggesting that ERM family members are directly associated with a putative integral membrane protein. On the other hand, radixin directly interacts with actin filaments at least in vitro (Tsukita et al., 1989), and the COOH-terminal half of ezrin is reportedly associated with actin filaments in vivo (Algrain et al., 1993).

Our previous findings suggesting the presence of ERM family members at cell to cell and cell to substrate adherens junctions is in sharp contrast with the recent report by Bretscher's group that at least ezrin and moesin are not concentrated at these junctions (Sato et al., 1992; Franck et al., 1993; Berryman et al., 1993). Previously, we used pAb and mAb that are not specific for each member, and those of Bretscher's group did not include the information about the localization of radixin, making it difficult to compare these data. Therefore, the presence of ERM family members at these junctions should be closely reevaluated using mAbs specific for each member, but as we previously reported, the marked masking problem for immunofluorescence microscopy is expected to hamper this type of localization work (Sato et al., 1992). This means that it is very difficult to speculate on the functions of ERM family members from their localization, especially to evaluate whether or not ERM family members are functionally involved in cell–cell and cell–substrate adhesion.

Thus, in this study, we directly analyzed the functions of ERM family members. We constructed antisense phosphorothioate oligonucleotides (PONs)[1] complementary to the sequence of each ERM family member and applied it to cultured epithelial (MTD-1A cells) and thymoma cells (L5178Y). Antisense PONs are so stable that they can effectively suppress the expression of corresponding proteins (Matsukura et al., 1987; Paria et al., 1992; Ratajczak et al., 1992; Yokozaki et al., 1993; Osen-Sand et al., 1993). When these cells were cultured in the presence of antisense PONs complementary to ezrin, radixin, or moesin sequences, the expression of each ERM family member was selectively suppressed. Immunofluorescence microscopy of these antisense-treated cells showed that all the members are colocalized at cell–cell adhesion sites, microvilli, and cleavage furrows; because of the reasons described above, in this paper, we use "cell–cell adhesion sites" instead of "cell to cell adherens junctions." We found that these antisense PONs perturbed cell–substrate adhesion, cell–cell adhesion, and microvilli formation. This perturbation was observed most clearly when the ezrin/radixin/moesin antisense PONs mixture was added to culture media. We believe this study will provide a basis for a better understanding of the significance of the coexpression of more than two ERM family members in single cells and of their physiological functions.

Materials and Methods

Antibodies

The mAb M11 was raised in a rat against recombinant mouse ezrin produced in *Escherichia coli* (see Fig. 3). The pAb II was raised in a rabbit against purified rat radixin (Tsukita et al., 1989), and the mAb M22 was raised in a rat against recombinant mouse moesin produced in *E. coli* (see Fig. 3). The mouse anti-ZO-1 mAb (T8-754) was previously reported (Itoh et al., 1991). Anti-mouse E-cadherin pAb was a gift from Dr. M. Takeichi (Kyoto University).

Cell Culture

The mouse mammary tumor MTD-1A cell line is a subclone isolated from the original MTD-1 line (Enami et al., 1984; Hirano et al., 1987). The mouse thymoma (L5178Y), mouse myeloma (P3), and mouse leukemia cell lines (WEHI231) were gifts from Dr. I. Yahara (Tokyo Metropolitan Institute for Medical Sciences), Dr. T. Obinata (Chiba University, Chiba, Japan), and Dr. T. Yamamoto (Tokyo University), respectively. MTD-1A cells were cultured in DME supplemented with 10% FCS, and the others were cultured in RPMI 1640 with 10% FCS. To minimize the amount of antisense PONs, 24- or 96-well plastic dishes or 16-well glass-bottomed chamber slide dishes (Nunc, Inc. Naperville, IL) were used.

For replating experiments of MTD-1A cells, cells cultured on dishes were incubated with 5 mM EDTA in PBS for 10 min followed by incubation with PBS containing 0.25% trypsin for 5 min. After floating cells were washed with culture medium, they were plated on culture dishes or glass coverslips in the same medium.

For Ca^{++}-switch experiments, MTD-1A cells were cultured in Eagle's minimal essential medium containing 0.05 mM Ca^{++} and 10% FCS (low Ca medium) for 48 h. The FCS in the low Ca medium was pretreated with chelex to remove Ca^{++} before use. They were then transferred to DME supplemented with 10% FCS (normal Ca medium).

Antisense PONs

First, two distinct positions, 1-24 and 301-324 (relative to the translation initiation site), of radixin sequence were chosen for the synthesis of antisense PONs, and we found that antisense PONs complementary to the former po-

1. *Abbreviations used in this paper*: AJ, adherens junction; FC, focal contacts; PONs, phosphorothioate oligonucleotides.

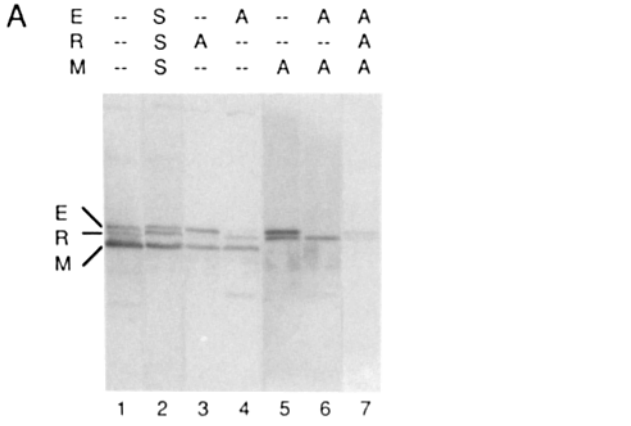

Figure 2. Effects of antisense PONs on the expression of the ERM family members in MTD-1A (*A*) and thymoma cells (*B*). MTD-1A and thymoma cells were cultured for 96 h in the presence of various combinations of ezrin, radixin, and moesin antisense/sense PONs in a 24-well dish, separated by SDS-PAGE, and immunoblotted with pAb 11, which recognizes all members of the ERM family by immunoblot (*E*, 85-kD ezrin; *R*, 82-kD radixin; *M*, 75-kD moesin). The same amount of cell extract was loaded for each sample. The combination of antisense (*A*) or sense (*S*) PONs is shown above each lane. Note that each antisense but not sense PONs selectively suppressed the expression of each ERM family member. In this system, ERM "single-suppressed" (lanes *3–5* in *A* and lanes *2–4* in *B*), "double-suppressed" (lane *6* in *A* and lane *5* in *B*), and "triple-suppressed" (lane *7* in *A* and lane *6* in *B*) cells were produced. In this figure, the suppressed bands are undetectable, but when the samples were overloaded, even at 96 h in culture, these suppressed bands are detectable by immunoblotting.

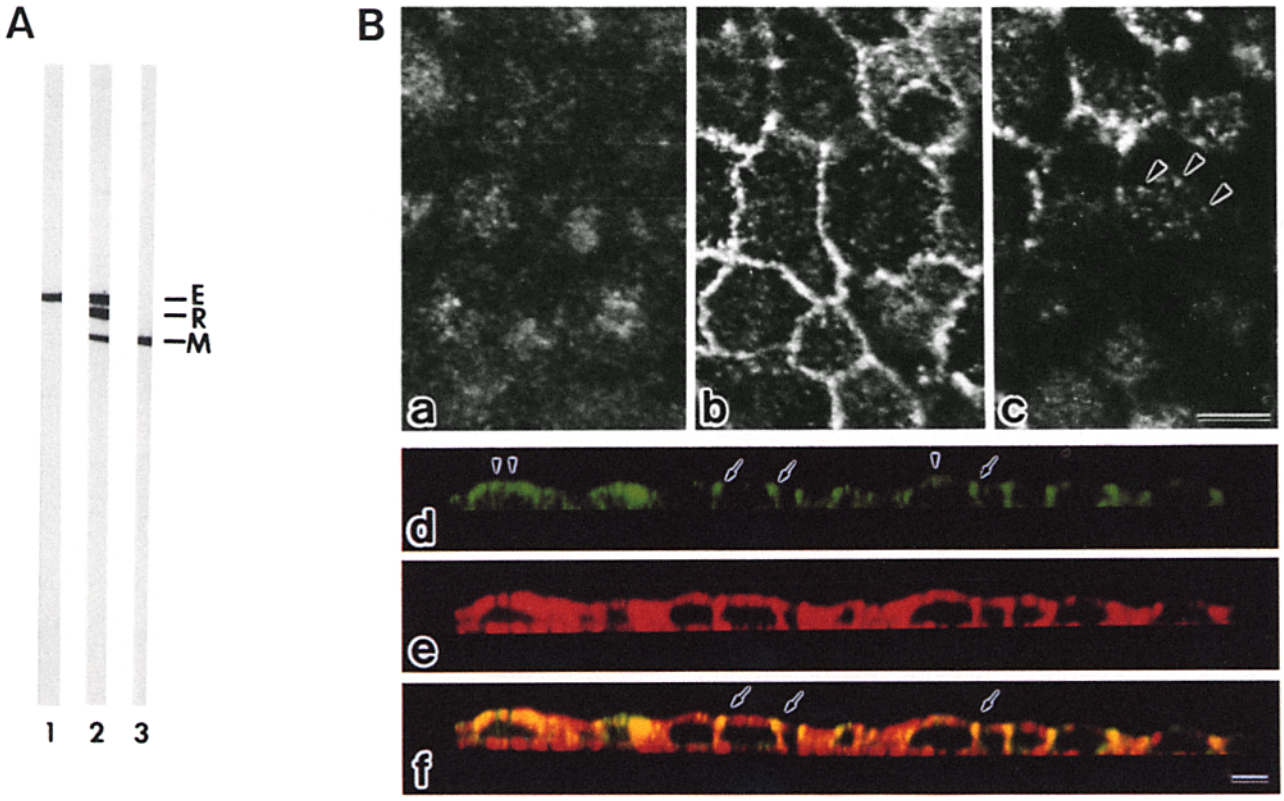

Figure 3. Characterization of antibodies. (*A*) Specificity of mAb M11 (lane *1*), pAb 11 (lane *2*), and mAb M22 (lane *3*) revealed by immunoblotting of MTD-1A cells. Note that in immunoblotting pAb 11 recognized ezrin (*E*) and moesin (*M*), as well as radixin (*R*), but that in immunofluorescence microscopy it appears to specifically react with radixin (see Fig. 4). This is probably caused by the difference in the sample treatment between immunoblotting and immunofluorescence microscopy; SDS treatment and formaldehyde-fixation, respectively. (*B*) Immunofluorescence staining pattern of MTD-1A cells with pAb 11 revealed by confocal microscopy. Confocal images of pAb 11–stained specimens at three focal planes (*a*, substratum level; *b*, junctional complex level; and *c*, upper surface level) reveal the antigen concentration in the cell–cell adhesion sites at the junctional complex level (*b*) and in the microvilli (*arrowheads*) at the upper surface level. This concentration at both levels (*arrows* and *arrowheads*, respectively) is also shown by the vertical section images of the samples (*d*). *e*, rhodamine-phalloidin staining; *f*, the merged image. Bars, 20 μm in *a–c* and 20 μm in *d–f*.

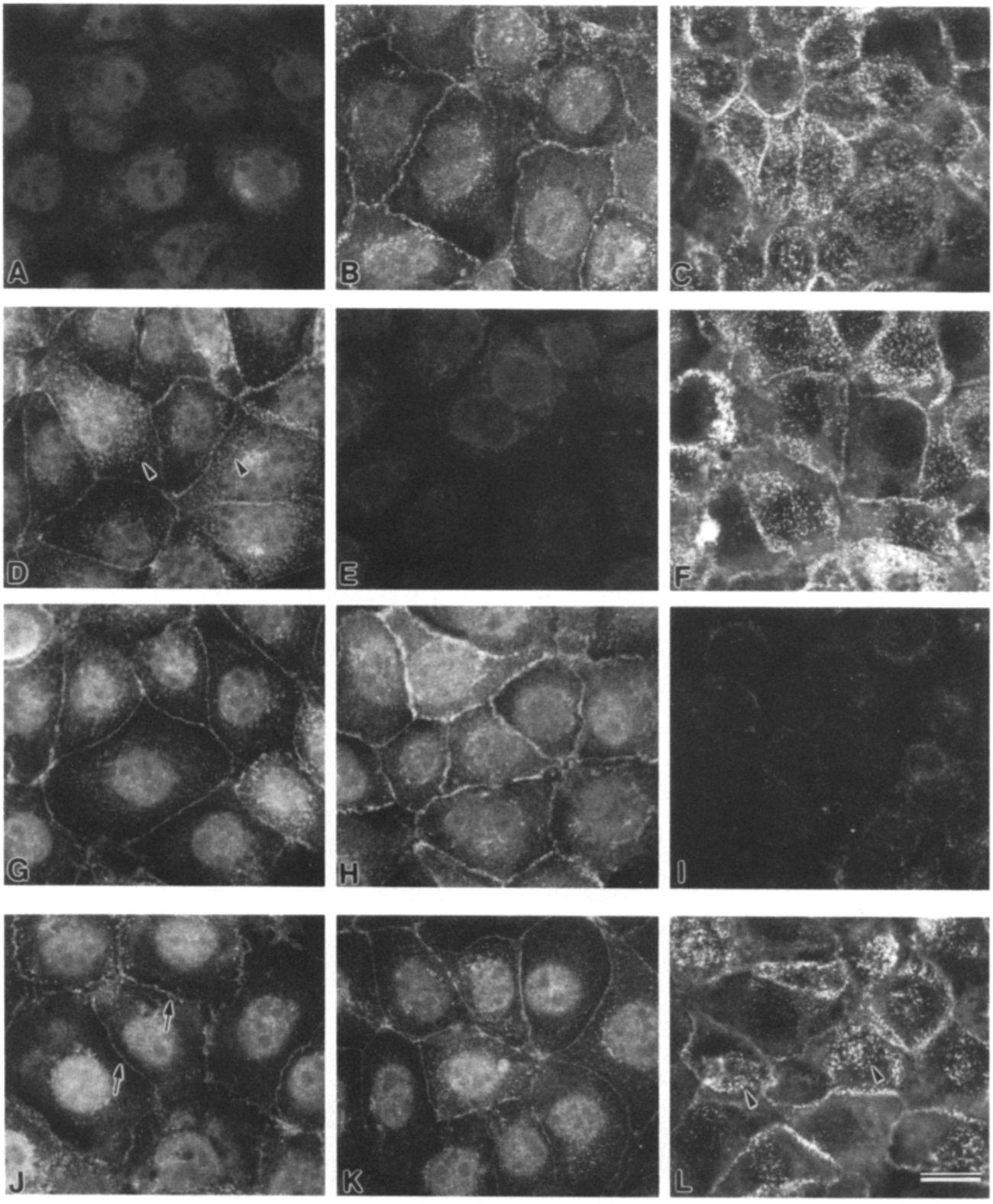

Figure 4. Distribution of ERM family members in antisense-treated MTD-1A cells. MTD-1A cells were cultured for 96 h in the presence of ezrin (*A–C*), radixin (*D–F*), or moesin (*G–I*) antisense PONs, or in the presence of the ezrin/radixin/moesin sense PONs mixture (*J–L*), and then immunofluorescently stained with antiezrin mAb M11 (*A*, *D*, *G*, and *J*), antiradixin pAb Il (*B*, *E*, *H*, and *K*), or antimoesin mAb M22 (*C*, *F*, *I*, and *L*). In sense-treated cells (*J-L*), all ERM family members are localized together at cell-cell adhesion sites (*arrows*) and microvilli on apical surfaces (*arrowheads*). Ezrin/radixin and moesin have a tendency to be to some extent sorted into cell–cell adhesion sites and microvilli, respectively. In ezrin/radixin (*A*, *B*, *D*, *E*, *G*, *H*, *J*, and *K*) and moesin (*C*, *F*, *I*, and *L*) staining, the focus plane is fixed at the level of cell–cell adhesion sites and of the apical surface, respectively. Even in ezrin/radixin staining, when the apical surface is focused, clear signals were detected from microvilli (e.g., *arrowheads* in *D*). Among antisense-treated cells, only in *A*, *E*, and *I*, immunofluorescence signals are very weak, and in *B–D* and *F–H*, there are no significant changes in the distribution of ERM family members. Staining of nuclei is nonspecific, since it was not affected by the antisense PONs. Bar, 20 μm.

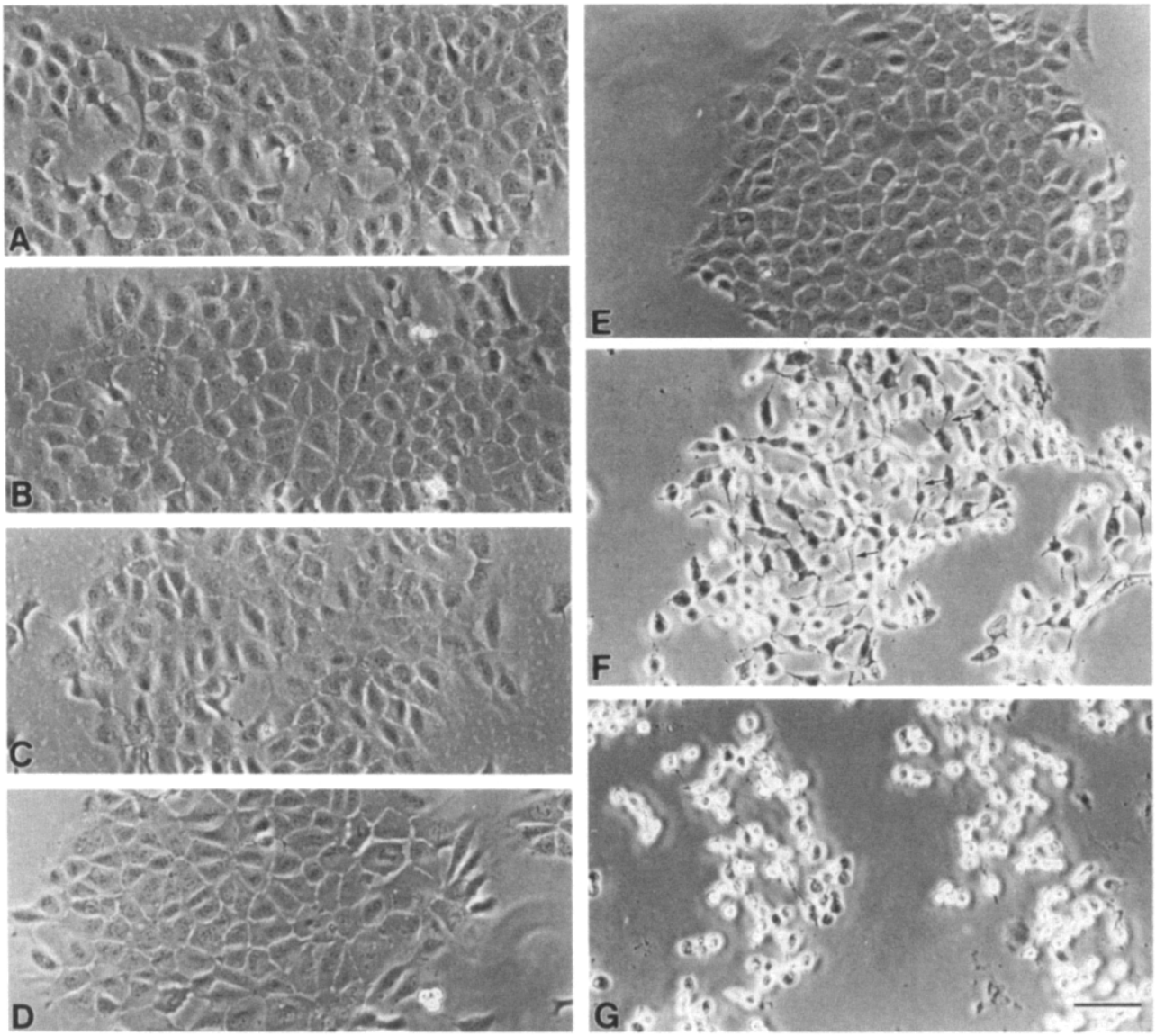

Figure 5. Effects of ERM family member antisense PONs on the cell–substrate adhesion of MTD-1A cells. When MTD-1A cells are cultured for 96 h in the presence of ezrin (*A*), radixin (*B*), or moesin (*C*) antisense PONs, or in the presence of the ezrin/radixin/moesin sense PONs mixture (*D*), no effects on the cell shape were detectable. In sharp contrast, the ezrin/radixin/moesin antisense PONs mixture induced significant morphological changes: At 24 h in culture (*E*), there were no structural changes, whereas at 48 h (*F*), the cells rounded up with very thin protrusions (*arrows*) followed by the complete detachment of cells from substratum at 60 h (*G*). Bar, 100 μm.

sition was highly effective. Therefore, we synthesized antisense PONs complementary to position 1-24 of the mouse ezrin, radixin, and moesin coding regions (see Fig. 1). Sense PONs corresponding to position 1-24 were synthesized as controls. All effects induced by antisense PONs in this study were totally canceled by the addition of 1.5 vol of sense PONs. The antisense PONs sequences did not have significant homology with any other sequences in the database. All experiments using antisense PONs were repeated three times, and the results obtained were essentially reproducible.

The antisense and sense PONs were synthesized on a synthesizer (model 392; Applied Biosystems, Inc., Foster City, CA) in our laboratory or in that of Takara Shuzo Co. (Kyoto, Japan), purified over Aquapore (RP-300; Applied Biosystems, Inc., Foster City, CA), ethanol precipitated, and taken up in media. In general, to effectively suppress the expression of structural proteins such as ERM family members, the concentration of antisense PONs in the medium must be maintained at a relatively high level for several days, probably because of their low turnover rate. In this study, we determined that antisense PONs should be added into the culture medium every 3–4 h at the concentration of 20 μM. In more detail, initially, antisense or sense PONs were added to the culture medium at the concentration of 20 μM, and at every 3–4 h, the same amount of PONs were added. After every four additions, the culture medium was exchanged with new medium containing 20 μM PONs. In this protocol, when the ezrin/radixin/moesin antisense PONs mixture was added, the combined concentration of PONs was 60 μM (3×20 μM). Therefore, to evaluate the possibility that the marked effects of the antisense PONs mixture are simply caused by differences in the total amount of PONs, in some experiments corresponding to Figs. 5 and 10, 60 μM ezrin, radixin, or moesin antisense PONs were added. The results obtained with such a high concentration of antisense PONs were the same as those obtained with 20 μM antisense PONs. Therefore, the data with 20 μM single antisense PONs were presented here.

Gel Electrophoresis and Immunoblotting

One-dimensional SDS-PAGE (10%) was based on the method of Laemmli (1970), and the gels were stained with Coomassie brilliant blue R-250 or silver staining kit (Wako Pure Chemical Industries, Osaka, Japan).

After electrophoresis, proteins were electrophoretically transferred from gels to nitrocellulose sheets, which were then incubated with the first anti-

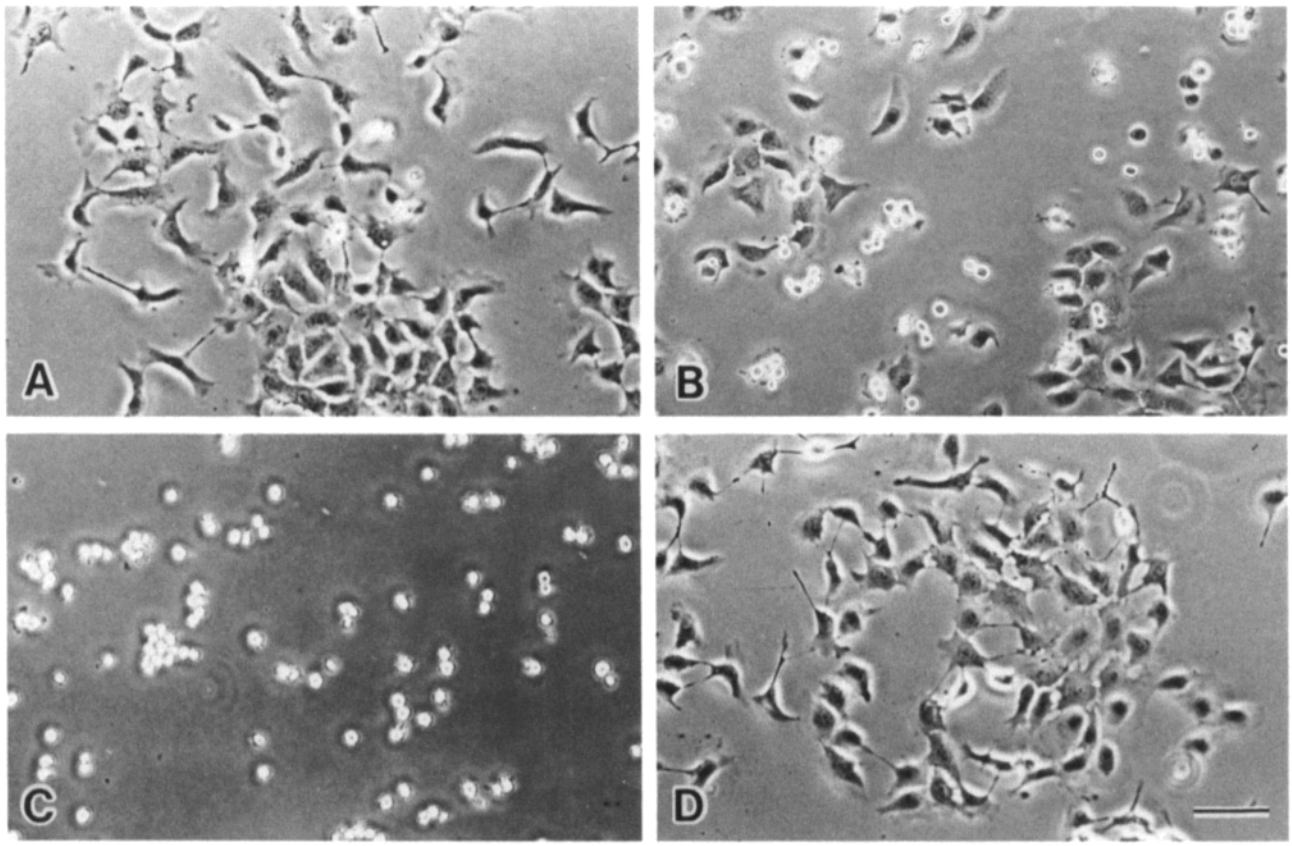

Figure 6. Effects of ERM family member antisense PONs on adhesion and spreading on the substratum after replating MTD-1A cells. MTD-1A cells were cultured for 48 h in the presence of the ezrin/radixin/moesin sense PONs mixture (*A*) or in the presence of ezrin (*B*), radixin (*C*), or moesin (*D*) antisense PONs, detached from the substratum by the use of EDTA and trypsin, then replated and cultured in plastic dishes for 15 h in the presence of the same PONs. Moesin antisense-treated cells (*D*) normally adhered to and spread over the dishes like sense-treated cells (*A*), while the ability for adhesion and spreading was suppressed partly in ezrin antisense-treated cells (*B*) and completely in radixin antisense-treated cells (*C*). Bar, 100 μm.

body. Antibodies were detected by means of a blotting detection kit (Amersham Corp., Arlington Heights, IL).

Immunofluorescence Microscopy

For indirect immunofluorescence microscopy, cells cultured on coverglasses or in glass-bottomed Chamber Slides (Nunc, Inc.) were fixed with 1% formaldehyde in PBS for 15 min at room temperature, then treated with 0.2% Triton X-100 in PBS for 10 min. After samples were treated with PBS containing 1% BSA for 10 min, they were incubated with the first antibody, washed with PBS, and then incubated with the second antibody. FITC-conjugated goat anti-rat IgG, FITC-conjugated goat anti-rabbit IgG (Tago, Inc., Burlingame, CA), and/or rhodamine-conjugated goat anti-mouse IgG (Chemicon International, Inc., Temecula, CA) were the second antibodies. Samples were then washed with PBS and then examined using a fluorescence microscope (Axiophoto photomicroscope; Carl Zeiss, Oberkochen, Germany) or a confocal laser scanning microscope (Laser Scan Microscope LSM 310; Carl Zeiss).

Scanning Electron Microscopy

Thymoma cells were placed on the poly-L-lysine-coated coverslips in RPMI medium for 5 min, then fixed with 0.2 M cacodylate buffer (pH 7.2) containing 2.5% glutaraldehyde and 2% formaldehyde at 4°C overnight followed by postfixation with the same buffer containing 1% OsO_4 at 4°C for 1 h. Samples were then washed with distilled water, dehydrated in a graded series of ethanol, transferred into isoamyl acetate, and dried in a critical point drier (Eiko Engineering, Ibaraki, Japan) after substitution with liquid CO_2. Dried samples were coated with gold by means of a gold sputter coater (Eiko Engineering), and were examined under a scanning electron microscope (model S-800; Hitachi Co., Ibaraki, Japan).

Results

Effects of Antisense Phosphorothioate Oligonucleotides on the Expression of ERM Family Members

By preliminary immunohistochemical analyses with cultured MTD-1A cells, we checked whether or not antisense PONs complementary to two distinct positions, 1-24 and 301-324 (relative to the translation initiation site), of the mouse radixin coding region suppress radixin expression. We found that when 20 μM antisense PONs complementary to position 1-24 of radixin sequence were added to the culture medium every 3–4 h, radixin expression appeared to be most effectively and continuously suppressed. Therefore, we synthesized antisense PONs complementary to position 1-24 of the mouse ezrin, radixin, and moesin coding regions (Fig. 1), and examined the effects of these antisense PONs on the expression of ERM family members in MTD-1A cells and thymoma cells by immunoblotting with pAb II (Fig. 2).

The pAb II recognizes all the ERM family members in immunoblotting (Sato et al., 1992). When MTD-1A cells were cultured in the presence of ezrin, radixin, or moesin antisense PONs, the expression of each ERM family member was selectively suppressed (Fig. 2 *A*, lanes *3–5*). Furthermore, the addition of the ezrin/moesin antisense PONs mix-

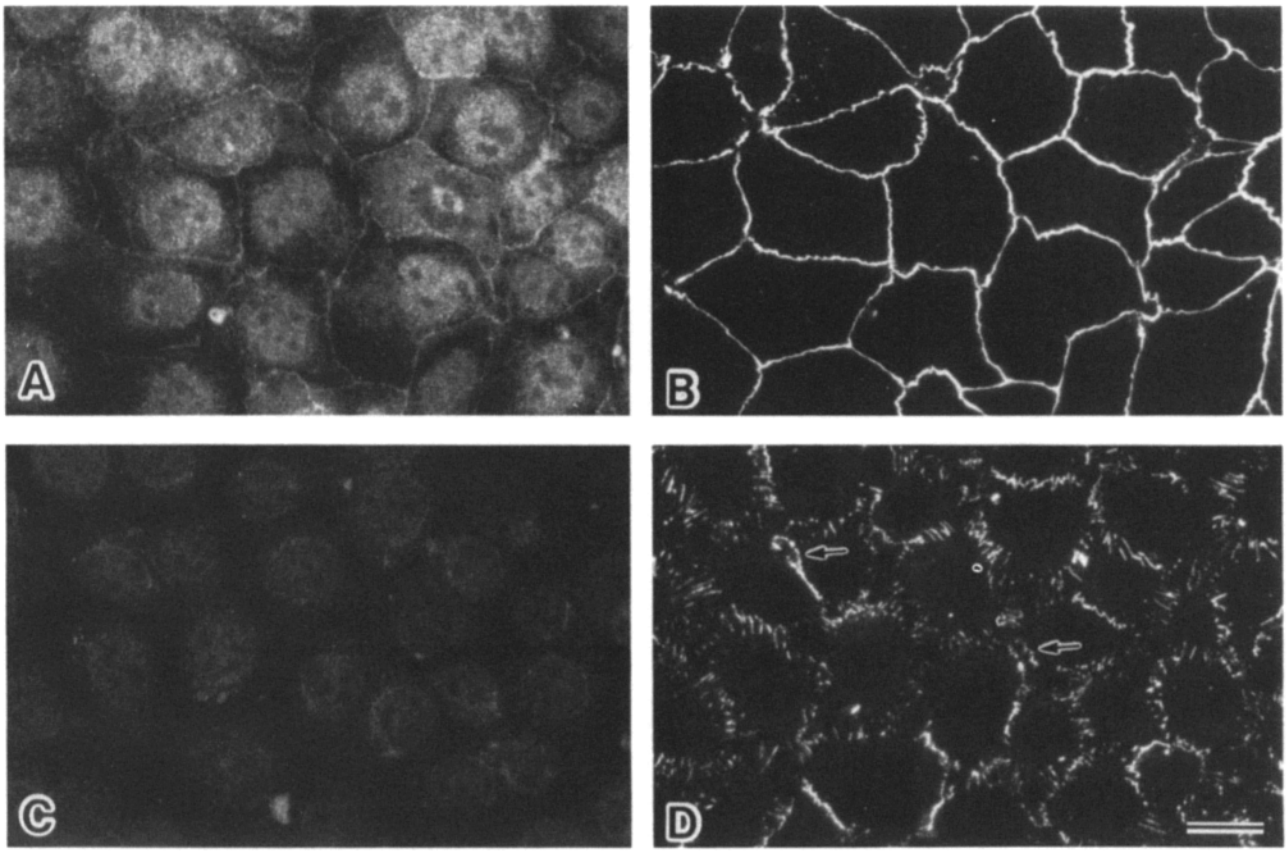

Figure 7. Effects of the ezrin/radixin/moesin antisense PONs mixture on the cell–cell adhesion in MTD-1A cells. As shown in Fig. 5 *E–G*, the ezrin/radixin/moesin antisense PONs mixture appears to affect not only cell–substrate adhesion, but also the cell-cell adhesion. At 30 h in culture in the presence of the ezrin/radixin/moesin sense PONs mixture (*A* and *B*) or the ezrin/radixin/moesin antisense PONs mixture (*C* and *D*), cells were doubly stained with antiradixin pAb I1 (*A* and *C*) and anti-ZO-1 mAb (*B* and *D*). Suppression of radixin expression (and also ezrin and moesin) (*C*) was accompanied by the destruction of cell-cell adhesion (*D*). The ZO-1 staining became discontinuous and occasionally split (*arrows*). Bar, 20 μm.

ture to the culture medium suppressed both ezrin and moesin expression, but did not affect that of radixin (Fig. 2 *A*, lane *6*). The expression of ERM family members was totally suppressed in the presence of the ezrin/radixin/moesin antisense PONs mixture (Fig. 2 *A*, lane *7*). The same results were obtained with thymoma cells (Fig. 2 *B*). In the presence of antisense PONs, the expression level of corresponding ERM family members appeared to decrease with time in a linear fashion, and as shown in Fig. 2, at 96 h in culture, their expression was almost undetectable by immunoblotting. However, even at 96 h, when the samples were overloaded on SDS-PAGE, the suppressed bands were detectable, and the degree of suppression gradually proceeded with culture time even after 96 h. In these types of experiments with antisense PONs, we should always keep it in mind that the antisense PONs can effectively suppress the expression of a protein but cannot completely suppress it. None of the sense PONs affected the expression of ERM family members either in MTD-1A or in thymoma cells. We could not find any clear cellular compensation for suppression of one ERM family member by increased synthesis or decreased turnover of another member, although some slight compensation appeared to be detected in some cases (for example, see in Fig. 2 *A*, lane *5*).

Next, the effects of antisense PONs on the expression of ERM family members in MTD-1A cells were examined by immunofluorescence microscopy. As will be shown later (see Fig. 5), the morphology of the "single-suppressed" cells was not significantly affected. We then immunofluorescently stained these ezrin, radixin, or moesin "single-suppressed" MTD-1A cells with three distinct antibodies: mAb M11 that was raised in rat against recombinant mouse ezrin, pAb I1 that was raised in rabbit against purified rat radixin, and mAb M22 that was raised in rat against recombinant mouse moesin (Fig. 3 *A*). In control MTD-1A cells, the confocal microscopy revealed that all these antibodies stained cell–cell adhesion sites at the the most apical level and microvilli at the apical surface (Fig. 3 *B*). Antiezrin mAb M11 and antiradixin pAb I1 stained cell–cell adhesion sites stronger than microvilli, whereas antimoesin mAb M22 showed a stronger staining in microvilli than in cell–cell adhesion sites. In dividing cells, the cleavage furrows were intensely stained by all these antibodies (data not shown). As shown in Fig. 4 *A–C*, in ezrin single-suppressed cells, antiezrin mAb M11 gave very weak signals, while antiradixin pAb I1 and antimoesin mAb M22 intensely stained cell–cell adhesion sites and microvilli. In contrast, in the radixin single-suppressed cells, the staining profile with antiezrin mAb M11 and an-

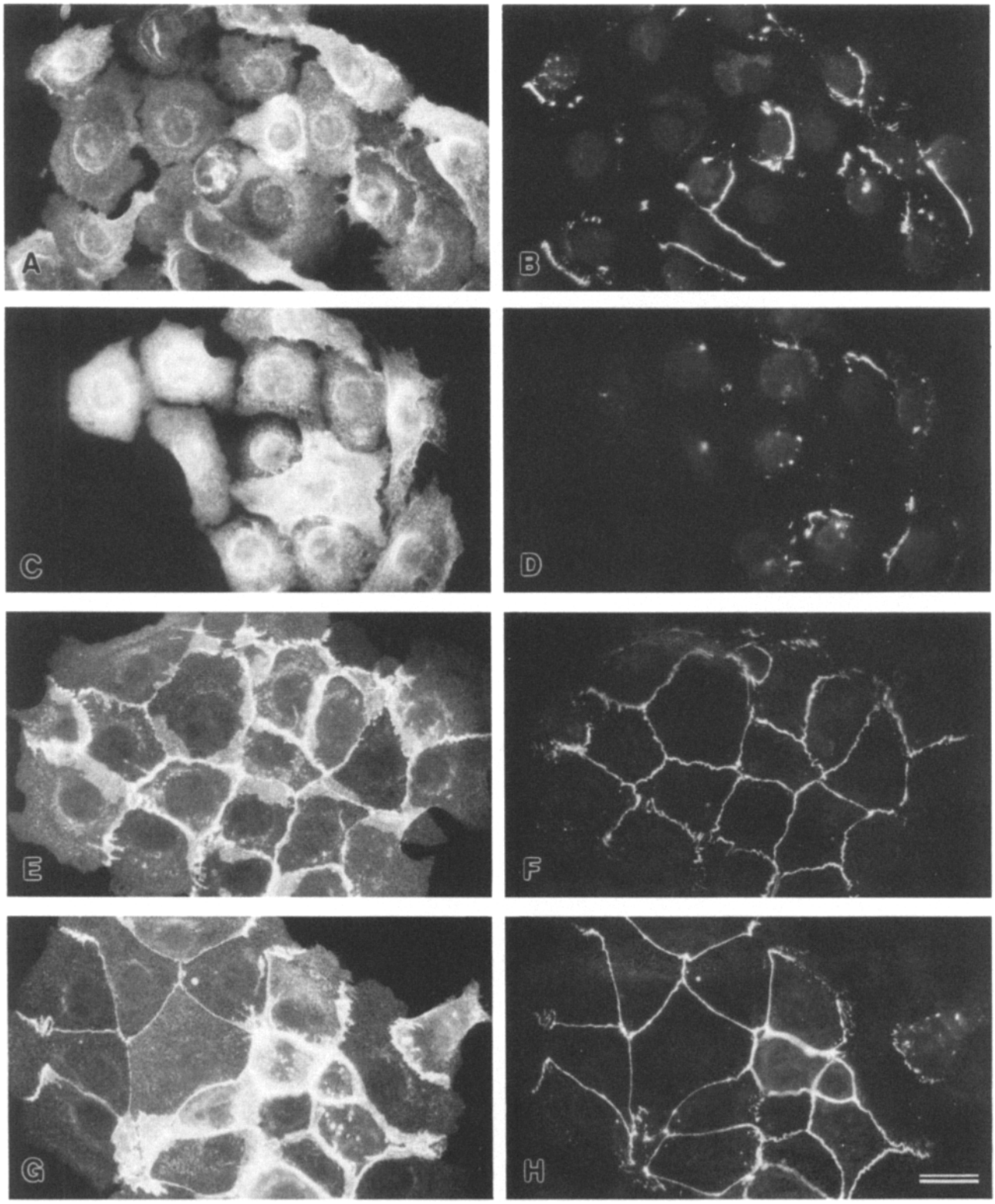

Figure 8. Effects of ERM family member antisense PONs on the formation of cell–cell adhesion in MTD-1A cells. In the low-Ca medium (0.05 mM Ca^{2+}), MTD-1A cells were cultured for 48 h in the presence of ezrin (*A* and *B*), radixin (*C* and *D*), or moesin (*E* and *F*) antisense PONs, or in the presence of the ezrin/radixin/moesin sense PONs mixture (*G* and *H*), then transferred to normal Ca medium (2 mM Ca^{2+}) in the presence of the same PONs. Twelve hours after the Ca switch, the cells were doubly stained with anti-E-cadherin pAb (*A*, *C*, *E*, and *G*) and anti-ZO-1 mAb (*B*, *D*, *F*, and *H*). E-cadherin and ZO-1 are concentrated at cell–cell adhesion sites in moesin antisense-treated (*E* and *F*), and in sense-treated cells (*G* and *H*), but it was hardly detectable in ezrin (*A* and *B*) and radixin (*C* and *D*) antisense-treated cells. Bar, 20 μm.

timoesin mAb M22 was not affected, while the staining with antiradixin pAb Il became very weak (Fig. 4 *D–F*). Furthermore, in moesin single-suppressed cells, only faint signals were detected with antimoesin mAb M22, while strong signals were evident at cell–cell adhesion sites and microvilli with antiezrin mAb M11 and antiradixin pAb Il (Fig. 4 *G–I*).

In summary, also at the immunofluorescence level, antisense PONs selectively suppressed the expression of each ERM family member without affecting the distribution of the other members. Conversely speaking, this indicates that the three antibodies used here, mAb M11, pAb Il, and mAb M22, are specific for ezrin, radixin, and moesin, respectively, at the immunofluorescence microscopic level. Also in immunoblotting, mAb M11 and mAb M22 specifically recognize ezrin and moesin, respectively, although pAb Il is not specific for radixin in immunoblotting (see Fig. 3 *A*). This strict specificity of antibodies at the "immunofluorescence level" led to the conclusion that at least in MTD-1A cells, ezrin, radixin, and moesin are colocalized at cell–cell adhesion sites, microvilli, and cleavage furrows, although ezrin/radixin and moesin appeared to be sorted, to some extent, to cell–cell adhesion sites and microvilli, respectively.

Perturbation of Cell–Substrate Adhesion by Antisense PONs

None of ezrin, radixin, moesin (Fig. 5, *A–C*), or any pair of the antisense PONs (data not shown) induced any morphological changes of MTD-1A cells. However, when MTD-1A cells were cultured in the presence of a mixture of ezrin/radixin/moesin antisense PONs, a significant change of cell shape was gradually induced (Fig. 5, *E–G*). Cells rounded up with very thin protrusions at ~48 h incubation, and began to float off from the substratum at ~60 h. These floating cells were viable judging from the trypan blue staining, and actin and vinculin were diffusely stained and observed by immunofluorescence microscopy (data not shown). The ezrin/radixin/moesin sense PONs mixture did not induce morphological changes of MTD-1A cells (Fig. 5 *D*). At 48 h, the morphological changes observed were completely reversible. Removal of the antisense PONs mixture at this timing resulted in the formation of normal cell–cell and cell–substrate adhesion (data not shown).

Next, we examined the effect of antisense PONs after replating on the attachment and spreading. MTD-1A cells were cultured for 48 h in the presence of ezrin, radixin, or moesin antisense PONs, floated off from the substratum using EDTA and trypsin, and then replated on the substratum in the presence of antisense PONs (Fig. 6). Cells treated singly with radixin antisense PONs completely lost the ability to attach and spread (Fig. 6 *C*), and ezrin antisense-treated cells seemed to partly lose the attachment ability (Fig. 6 *B*). In sharp contrast, moesin antisense-treated cells attached normally and spread on the substratum (Fig. 6 *D*). The ezrin/radixin/moesin sense PONs mixture did not affect these properties (Fig. 6 *A*). All effects of antisense PONs in replating experiments were reversible.

Perturbation of Cell–Cell Adhesion by Antisense PONs

As shown in Fig. 5 *E–G*, the ezrin/radixin/moesin antisense PONs mixture appears to affect not only the cell–substrate adhesion, but also cell–cell adhesion. These antisense-treated cells were doubly stained with antiradixin pAb Il and anti–ZO-1 mAb just before the cell changed shape (Fig. 7). The destruction of cell–cell adhesion proceeds or is simultaneously associated with that of cell–substrate adhesion. Any one or pair of the three antisense PONs failed to affect the cell–cell adhesion (data not shown).

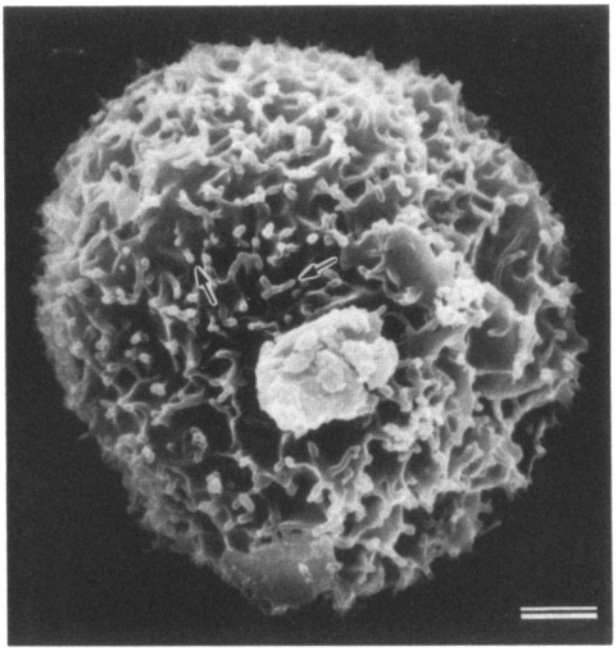

Figure 9. Scanning electron microscopy of thymoma cells incubated with the ezrin/radixin/moesin sense mixture for 6 d. Cells are characterized by a large number of microvilli on their cell surface (*arrows*). Bar, 1 μm.

We then examined whether or not these antisense PONs individually affect the formation of cell–cell adhesion when cells are transferred from low to normal Ca medium. MTD-1A cells were cultured for 2 d in the low Ca medium containing 0.05 mM Ca^{++} in the presence of ezrin, radixin, or moesin antisense PONs, then transferred to the normal Ca medium containing 2 mM Ca^{++} in the presence of antisense PONs. In the presence of ezrin or radixin antisense PONs, the concentration of E-cadherin and ZO-1 at cell–cell contact sites was significantly inhibited (Fig. 8, *A–D*), whereas moesin anti-sense PONs did not affect these proteins (Fig. 8, *E* and *F*). The ezrin/radixin/moesin sense PONs mixture did not affect the formation of cell–cell adhesion (Fig. 8, *G* and *H*).

Effects of Antisense PONs on Microvilli in Thymoma Cells

The length and number of microvilli of MTD-1A cells varied depending on their cell cycle. Therefore, to examine the effects of antisense PONs on microvillus structures, we used mouse thymoma cells (L5178Y), which bear a large number of microvilli and do not show significant cell cycle-dependent changes of microvillus appearance (Fig. 9).

As shown in Fig. 10, *A* and *B* by scanning electron micros-

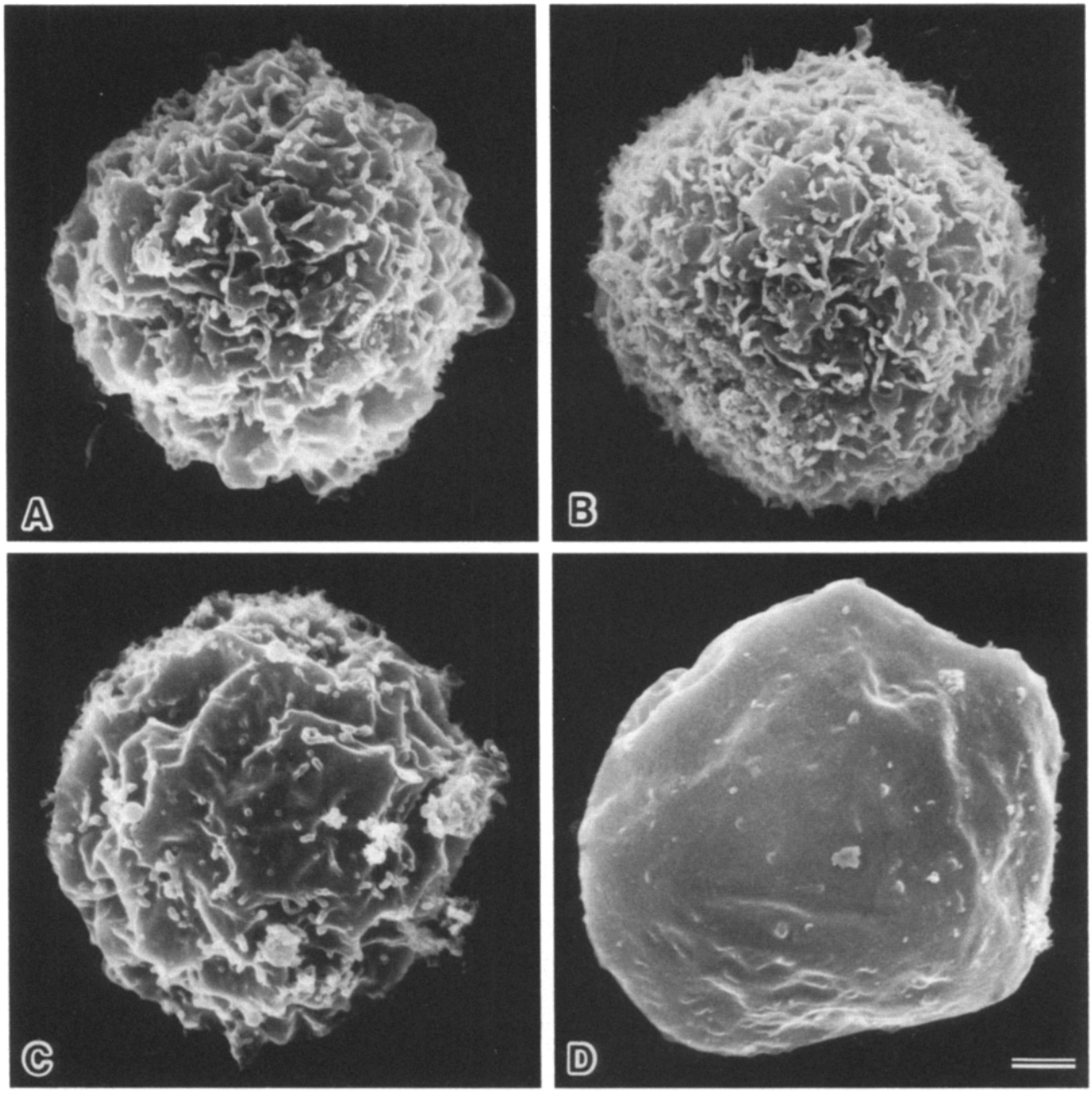

Figure 10. Effects of ERM family member antisense PONs on the microvilli structure of thymoma cells. Thymoma cells were cultured for 6 d in the presence of ezrin (*A*), radixin (*B*), or moesin (*C*) antisense PONs, or in the presence of the ezrin/radixin/moesin antisense PONs mixture (*D*). Microvilli were not affected by ezrin (*A*) and radixin (*B*) antisense PONs, whereas moesin antisense PONs partly affected them (*C*). In the presence of the mixture of antisense PONs, microvilli completely disappeared, leaving a smooth cell surface (*D*). Bar, 1 μm.

copy, when thymoma cells were cultured in the presence of ezrin or radixin antisense PONs, no change was detected in the length and number of microvilli even 6 d after the beginning of antisense exposure. Moesin antisense PONs individually appeared to decrease the number and length of microvilli of 6-d cultures, but the extent of this effect varied from cell to cell (Fig. 10 *C*). In sharp contrast, the addition of the ezrin/radixin/moesin antisense PONs mixture clearly affected the microvilli structures (Fig. 10 *D*). 4 d after exposure, microvilli began to decrease in number and length (Fig. 11, *A* and *B*). At 6 d, all cells were completely devoid of microvilli (Figs. 10 *D* and 11 *C*). This time course of the microvilli disappearance appeared to be similar to that of the suppression of the ERM expression detected by immunofluorescence microscopy (Fig. 12). Trypan blue staining revealed that these cells were viable. With the ezrin/radixin/moesin sense PONs mixture, all cells bore a large number of microvilli (Fig. 9). The same results were obtained using mouse myeloma P3 and mouse leukemia WEHI231 cells (data not shown). At 4 d, removal of the antisense PONs

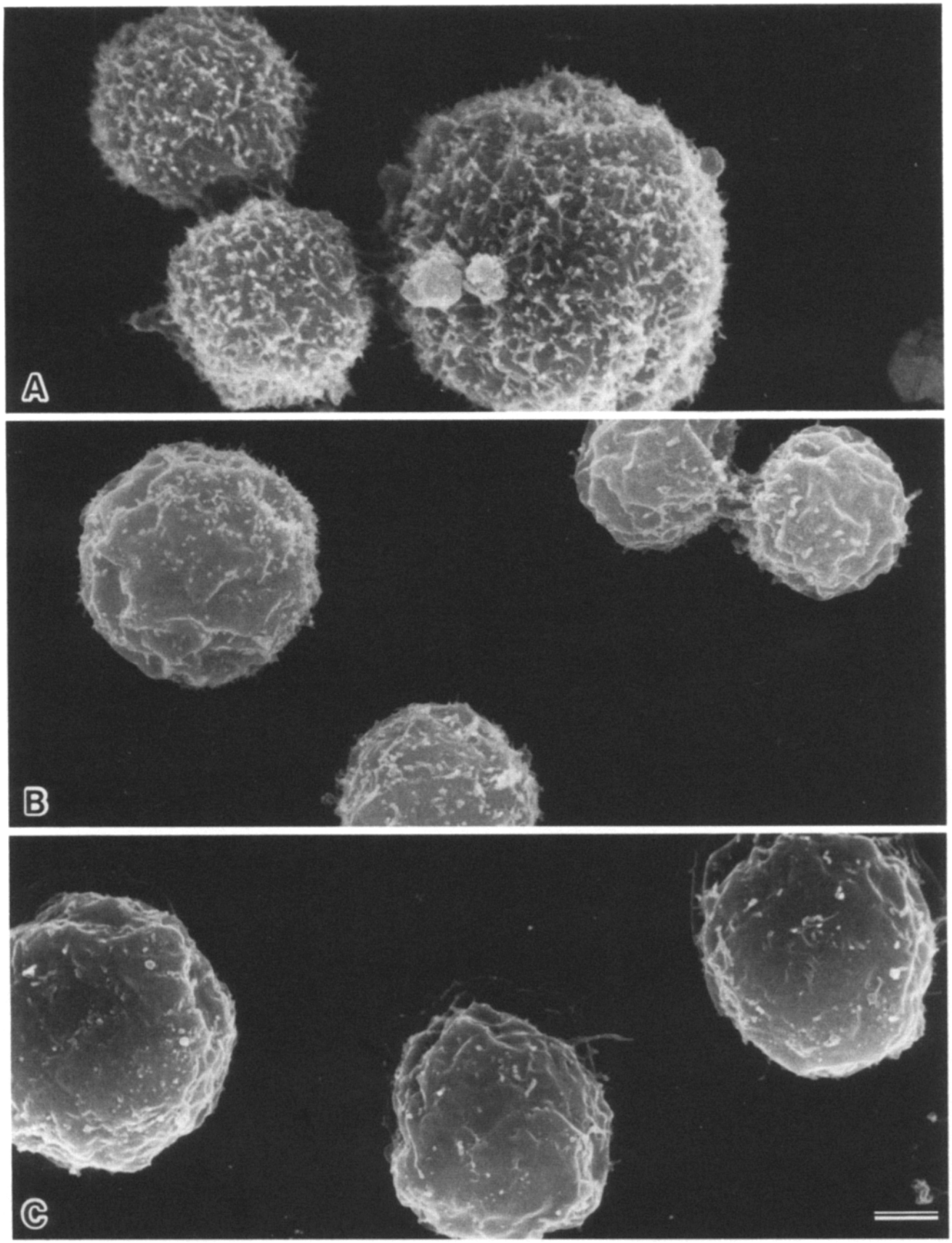

Figure 11. Scanning electron microscopy showing time course of the disappearance of microvilli of thymoma cells induced by the ezrin/radixin/moesin antisense PONs mixture. Although at the beginning of the treatment no structural changes were seen in microvilli (*A*), they began to decrease in number and length after 4 d in culture (*B*). After 6 d, all cells were completely devoid of microvilli (*C*). Bar, 2 μm.

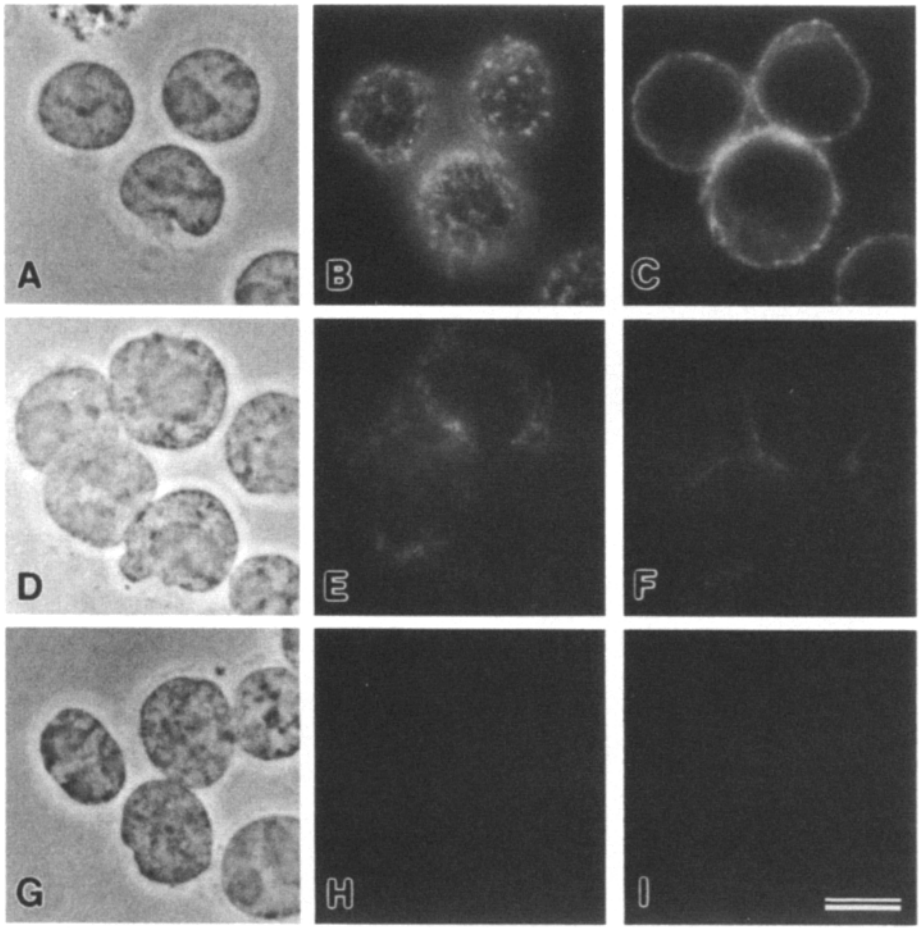

Figure 12. Immunofluorescence microscopy showing time course of the suppression of ERM expression in thymoma cells induced by the ezrin/radixin/moesin antisense PONs mixture. Phase contrast images (*A*, *D*, and *G*), and immunofluorescence images with the mixture of mAb M11, pAb Il, and mAb M22, focused at the surface (*B*, *E*, and *H*) and the center (*C*, *F*, and *I*) of cells. At the beginning of antisense exposure, microvilli-like structures on the cell surface were intensely stained (*A–C*), while at 4 d in culture, the staining signals became weak but clear (*D–F*). After 6 d, the cells were hardly stained (*G–I*). Bar, 5 μm.

mixture resulted in the reappearance of microvilli, while at 6 d in most cells, the morphological changes (i.e., the disappearance of microvilli) appeared to be irreversible.

Discussion

We examined effects of ezrin, radixin, and moesin antisense PONs on the morphology of cultured cells such as MTD-1A and thymoma cells (L5178Y). The ERM family members are highly homologous in their amino acid sequences (>70% identity). Nevertheless, the antisense PONs selectively suppressed the expression of each member of the ERM family. Therefore, this system enabled us to analyze in detail the function of each.

Using this system, we produced ezrin, radixin, or moesin single-suppressed MTD-1A cells. In these cells, the suppression of one member did not affect the localization of the other two; they were concentrated at cell–cell adhesion sites, microvilli, and cleavage furrows. Furthermore, "double-suppressed" cells, for example ezrin(−)/radixin(−)/moesin(+) cells, were also produced. Even in these cells, the expressed ERM family member showed the same subcellular distribution, indicating that each member by itself can concentrate at these sites. ERM family members are thought to be directly associated with integral membrane proteins (Gould et al., 1989; Turunen et al., 1989; Funayama et al., 1991; Lankes and Furthmayr, 1991). If all the members share the same membrane protein, their redundant colocalization observed here would be easily explained. However, this interpretation may be oversimplified, because as shown in this study, ezrin/radixin and moesin are sorted to some extent in MTD-1A cells.

The present study revealed the functional involvement of ERM family members both in cell–cell and cell–substrate adhesion. The effects of their reduced expression on cell adhesion may be mediated by the changes in the actin filament/plasma membrane interaction (Sato et al., 1991), and not by the changes in the expression of adhesion molecules and their directly associated proteins. For example, we confirmed that the expression of cadherin, α catenin, and ZO-1 was not influenced by the treatment with antisense PONs (data not shown). Two points should be highlighted concerning perturbed cell adhesion. The first is that ERM family members appear to be involved preferably in the initial step of the formation of cell–substrate/cell–cell adhesion rather than in the maintenance of preformed adhesion. No single or pair of antisense PONs destroyed the preformed cell–substrate and cell–cell adhesion, whereas the ezrin or radixin single-suppressed cells showed a decreased ability not only to attach and spread on the substratum when replated but also to adhere to each other when transferred from low to normal Ca medium. Of course, the occurrence

of at least one member is required for the maintenance of preformed cell adhesion, because the addition of ezrin/radixin/moesin antisense PONs mixture completely destroyed both the preformed cell–substrate and cell–cell adhesion (see Figs. 5 and 7).

The second point to be highlighted is that the physiological role of moesin appears to be slightly different from that of ezrin and radixin. Actually, unlike the ezrin and radixin single-suppressed cells, the moesin single-suppressed cells normally attached and spread on the substratum when replated, and adhered to each other when transferred from low to normal Ca medium. However, moesin is somehow involved in cell adhesion because the ezrin/radixin antisense PONs mixture did not affect the preformed cell adhesion, whereas the ezrin/radixin/moesin antisense PONs mixture destroyed it completely. Therefore, it is likely that between ezrin/radixin and moesin, there is some synergetic interaction in the regulation of cell adhesion. In this context, it should be mentioned that among the ERM family members only moesin lacks the polyproline stretch at the COOH-terminal region (Lankes and Furthmayr, 1991; Sato et al., 1992), and that at least in MTD-1A cells, the localization of moesin is slightly different from that of ezrin/radixin.

As compared with cell adhesion, the microvillus appeared to be more resistant to the antisense PONs. After 3–4 d of culture in the presence of the ezrin/radixin/moesin antisense PONs mixture, microvilli gradually decreased in number and length, and only at 6 d did they completely disappear. As compared with the perturbation of cell adhesion, the complete suppression of ERM family members appears necessary for the disappearance of microvilli. This was most clearly observed in thymoma cells, but similar results were obtained using WEHI231 leukemia and P3 myeloma cells (data not shown).

Considering that ERM family members are concentrated at cleavage furrows (Sato et al., 1991; Yonemura et al., 1993), antisense PONs to ERM family members were expected to affect cytokinesis, resulting in the increase in number of cells with more than two nuclei. However, as far as we examined, the cells with two nuclei were hardly observed. As shown in Fig. 11 *B*, even 4 d after exposure to the ezrin/radixin/moesin antisense PONs mixture, dividing thymoma cells were observed, although the number was very small. When these cells were stained with anti-ERM antibodies, a weak but clear signal was detected from the surface of all cells (Fig. 12, *D–F*). However, at 6 d, all cells were completely devoid of microvilli and the ERM staining signal (Figs. 11 *C* and 12, *G–I*), and the dividing cells were hardly observed. These may indicate that the complete suppression of the ERM family members is required to affect cytokinesis, and that under such a complete suppression, not only the cytokinesis, but also the other stages of the cell cycle appears to be stopped, resulting in no dividing cells and no cells with two nuclei. A different approach will be required to experimentally clarify the functions of ERM family members in cytokinesis.

Finally, we should compare the present findings with those reported recently by Bretscher's group. They reported that in tissues ezrin and moesin exhibited very different cellular distributions (Berryman et al., 1993). Also using our antibodies, we confirmed this conclusion (Kasahara et al., unpublished data). On the other hand, in cultured cells, here we concluded that all the members of the ERM family are coexpressed and colocalized. Bretscher's group also reported the colocalization of ezrin and moesin in cultured cells (Franck et al., 1993). The apparent difference between their conclusions and ours is on the occurrence of ERM family members at cell–cell adherens junctions (AJ). As Figs. 3 *B* and 4 show, in MTD-1A cells, the specific ERM staining at the intercellular junctional area was clear. By contrast, Franck et al. (1993) concluded that ezrin and moesin are not concentrated at the cell–cell adhesion sites, although their confocal images appear to reveal the ezrin concentration at cell–cell adhesion sites of cultured A431 cells (see Fig. 8 in Frank et al., 1993). It is more difficult to determine whether ERM family members are present at the cell–substrate AJ, focal contacts (FC). We detected the staining with pAb 11 at FC after the treatment of cells to unmask antigenic sites (Sato et al., 1991), whereas Franck et al. (1993) found no ezrin or moesin there under the same condition. This discrepancy can be explained, given that only radixin is localized at FC, but it is also possible that during unmasking, some soluble members are artifactually bound to FC. To explain these discrepancies, further detailed localization work with specific mAbs is required, but this will not be easy because of the masking problem (Sato et al., 1991). Analysis of the cells microinjected with fluorescein-labeled recombinant ERM family members should help solve this problem. The present findings indicate the functional involvement of ERM family members in the AJ formation and support the view that ERM family members occur at AJ.

Our present results favored the notion that the coexpression of ERM family members, especially of ezrin and radixin, in single cells is a safety measure. This type of redundancy generally interferes with the analysis of protein functions, but as shown here, antisense PONs are very convenient tools with which to circumvent this. Therefore we conclude that ERM family members are involved at least in cell adhesion and microvilli formation. Further detailed analyses of the structures and functions of the ERM family members using single-suppressed, double-suppressed, and triple-suppressed cells will lead to a better understanding of how ERM family mediated actin filament/plasma membrane interactions are involved in cell adhesion, cell proliferation, and signal transduction.

We thank all the members of our laboratory (Laboratory of Cell Biology, National Institute for Physiological Sciences) for their helpful discussions. We would like to express our appreciation to Mr. A. Ohba and Mr. H. Maebashi (Laboratory of Electron Microscopy, National Institute for Physiological Sciences) for their assistance in scanning electron microscopy, and to Mrs. Y. Takeuchi for her excellent technical assistance. Our thanks are also due to Dr. M. Takeichi (Kyoto University) and Dr. I. Yahara (Tokyo Metropolitan Institute for Medical Sciences) for their gifts of anti-E-cadherin pAb and the thymoma cell line L5178Y, respectively.

This work was supported by research grants from the Ministry of Education, Science and Culture of Japan, and the Ministry of Health and Welfare of Japan.

Received for publication 7 October 1993 and in revised form 4 March 1994.

References

Algrain, M., O. Turunen, A. Vaheri, D. Louvard, and M. Arpin. 1993. Ezrin contains cytoskeleton and membrane binding domains accounting for its proposed role as a membrane-cytoskeletal linker. *J. Cell Biol.* 120:129–140.

Anderson, R. A., and R. E. Lovrien. 1984. Glycophorin is linked by band 4.1 protein to the human erythrocyte membrane skeleton. *Nature (Lond.).* 307:655–658.

Anderson, R. A., and V. T. Marchesi. 1985. Regulation of the association of membrane skeletal protein 4.1 with glycophorin by a polyphosphoinositide. *Nature (Lond.).* 318:295–298.

Berryman, M., Z. Franck, and A. Bretscher. 1993. Ezrin is concentrated in the apical microvilli of a wide variety of epithelial cells, whereas moesin is found primarily in endothelial cells. *J. Cell Sci.* 105:1025–1043.

Bretscher, A. 1983. Purification of an 80,000-dalton protein that is a component of the isolated microvillus cytoskeleton, and its localization in nonmuscle cells. *J. Cell Biol.* 97:425–432.

Bretscher, A. 1989. Rapid phosphorylation and reorganization of ezrin and spectrin accompany morphological changes induced in A-431 cells by epidermal growth factor. *J. Cell Biol.* 108:921–930.

Conboy, J., Y. W. Kan, S. B. Shohet, and N. Mohandas. 1986. Molecular cloning of protein 4.1, a major structural element of the human erythrocyte membrane skeleton. *Proc. Natl. Acad. Sci. USA.* 83:9512–9516.

Doolittle, R. F. 1984. *In* The Plasma Proteins. Vol. IV. F. W. Putnam, editor. Academic Press, Orlando, FL. pp. 317–360.

Enami, J., S. Enami, and M. Koga. 1984. Isolation of an insulin-responsive preadipose cell line and a mammary tumor-producing, dome-forming epithelial cell line from a mouse mammary tumor. *Dev. Growth & Differ.* 26:223–234.

Franck, Z., R. Gary, and A. Bretscher. 1993. Moesin, like ezrin, colocalizes with actin in the cortical cytoskeleton in cultured cells, but its expression is more variable. *J. Cell Sci.* 105:219–231.

Funayama, N., A. Nagafuchi, N. Sato, Sa. Tsukita, and Sh. Tsukita. 1991. Radixin is a novel member of the band 4.1 family. *J. Cell Biol.* 115:1039–1048.

Gould, K. L., A. Bretcher, F. S. Esch, and T. Hunter. 1989. cDNA cloning and sequencing of the protein-tyrosine kinase substrate, ezrin, reveals homology to band 4.1. *EMBO (Eur. Mol. Biol. Organ.) J.* 8:4133–4142.

Gould, K. L., J. A. Cooper, A. Bretscher, and T. Hunter. 1986. The protein-tyrosine kinase substrate, p81, is homologous to a chicken microvillar core protein. *J. Cell Biol.* 102:660–669.

Gu, M., J. D. York, I. Warshawsky, and P. W. Majerus. 1991. Identification, cloning, and expression of a cytosolic megakaryocyte protein-tyrosine-phosphatase with sequence homology to cytoskeletal protein 4.1. *Proc. Natl. Acad. Sci. USA.* 88:5867–5871.

Hirano, S., A. Nose, K. Hatta, A. Kawakami, and M. Takeichi. 1987. Calcium-dependent cell-cell adhesion molecules (cadherins): subclass specificities and possible involvement of actin bundles. *J. Cell Biol.* 105:2051–2510.

Hunter, T., and J. A. Cooper. 1981. Epidermal growth factor induces rapid tyrosine phosphorylation of proteins in A431 human tumor cells. *Cell.* 24:741–752.

Hunter, T., and J. A. Cooper. 1983. Role of tyrosine phosphorylation in malignant transformation by viruses and in cellular growth control. *Prog. Nucleic Acid Res. Mol. Biol.* 29:221–233.

Itoh, M., S. Yonemura, A. Nagafuchi, Sa. Tsukita, and Sh. Tsukita. 1991. A 220-kD undercoat-constitutive protein: its specific localization at cadherin-based cell-cell adhesion sites. *J. Cell Biol.* 115:1449–1462.

Lankes, W., and H. Furthmayr. 1991. Moesin: a member of the protein 4.1-talin-ezrin family of proteins. *Proc. Natl. Acad. Sci. USA.* 88:8297–8301.

Lankes, W., A. Griesmacher, J. Grunwald, R. Schwartz-Albiez, and R. Keller. 1988. A heparin-binding protein involved in inhibition of smooth-muscle cell proliferation. *Biochem. J.* 251:831–842.

Laemmli, U. K. 1970. Cleavage of structural proteins during the assembly of the head of bacteriophage T4. *Nature (Lond.).* 227:680–685.

Leto, T. L., I. Correas, T. Tobe, R. A. Anderson, and W. C. Horne. 1986. *In* Membrane Skeleton and Cytoskeletal Membrane Associations. V. Bennet, C. M. Cohen, S. E. Lux, and J. Palek, editors. Alan R. Liss, New York. pp. 201–209.

Matsukura, M., K. Shinozuka, G. Zon, H. Mitsuya, M. Reitz, J. S. Cohen, and S. Broder. 1987. Phosphorothioate analogs of oligodexynucleotides: inhibitors of replication and cytopathic effects of human immunodeficiency virus. *Proc. Natl. Acad. Sci. USA.* 84:7706–7710.

Osen-Sand, A., M. Catsicas, J. K. Stapie, K. A. Jones, G. Ayala, J. Knowles, G. Grenningloh, and S. Catsicas. 1993. Inhibition of axonal growth by SNAP-25 antisense oligonucleotides in vitro and in vivo. *Nature (Lond.).* 364:445–448.

Pakkanen, R., K. Hedman, O. Turunen, T. Wahlstrom, and A. Vaheri. 1987. Microvillus-specific M_r 75,000 plasma membrane protein of human choriocarcinoma cells. *J. Histochem. Cytochem.* 135:809–816.

Paira, B. C., S. K. Dey, and G. K. Andrews. 1992. Antisense c-*myc* effects on preimplantation mouse embryo development. *Proc. Natl. Acad. Sci. USA.* 89:10051–10055.

Ratajczak, M. Z., J. A. Kant, S. M. Luger, N. Hijiya, J. Zhang, G. Zon, and A. M. Gewirtz. 1992. In vivo treatment of human leukemia in a scid mouse with c-*myb* antisense oligonucleotides. *Proc. Natl. Acad. Sci. USA.* 89: 11823–11827.

Rees, D. J. G., S. E. Ades, S. J. Singer, and R. O. Hynes. 1990. Sequence and domain structure of talin. *Nature (Lond.).* 347:685–689.

Sato, N., N. Funayama, A. Nagafuchi, S. Yonemura, Sa. Tsukita, and Sh. Tsukita. 1992. A gene family consisting of ezrin, radixin, and moesin. Its specific localization at actin filament/plasma membrane association sites. *J. Cell Sci.* 103:131–143.

Sato, N., S. Yomemura, T. Obinata, Sa. Tsukita, and Sh. Tsukita. 1991. Radixin, a barbed end-capping actub-modulating protein, its concentrated at the cleavage furrow during cytokinesis. *J. Cell Biol.* 113:321–330.

Tsukita, Sa., Y. Hieda, and Sh. Tsukita. 1989. A new 82 kD-barbed end capping protein localized in the cell-to-cell adherens junction: purification and characterization. *J. Cell Biol.* 108:2369–2382.

Tsukita, Sh., Sa. Tsukita, A. Nagafuchi, and S. Yonemura. 1992. Molecular linkage between cadherins and actin filaments in cell-to-cell adherens junctions. *Curr. Opin. Cell. Biol.* 4:834–839.

Turunen, O., R. Winqvist, R. Pakkanen, K.H. Grzeschik, T. Wahlstrom, and A. Vaheri. 1989. Cytovillin, a microvillar M_r 75,000 protein. cDNA sequence, pro-karyotic expression, and chromosomal localization. *J. Biol. Chem.* 264:16727–16732.

Yang, Q., and N. K. Tonks. 1991. Isolation of a cDNA clone encoding a human protein-tyrosine phosphatase with homology to the cytoskeletal-associated proteins band 4.1, ezrin, and talin. *Proc. Natl. Acad. Sci. USA.* 88: 5949–5953.

Yokozaki, H., A. Budillon, G. Tortora, S. Meissner, S. L. Beaucage, K. Miki, and Y. S. Cho-Chung. 1993. An antisense oligodeoxynucleotide that depletes RI alpha subunit of cyclic AMP-dependent protein kinase induces growth inhibition in human cancer cells. *Cancer Res.* 15:868–872.

Yonemura, S., A. Nagafuchi, N. Sato, and Sh. Tsukita. 1993. Concentration of an integral membrane protein CD43 (leukosialin, sialophorin), in the cleavage furrow through the interaction of its cytoplasmic domain with actin-based cytoskeleton. *J. Cell Biol.* 120:437–449.